

Accelerated Syntheses of Porous Isostructural Lanthanide–Benzenetricarboxylates (Ln–BTC) Under Ultrasound at Room Temperature

Nazmul Abedin Khan,^[a] Md. Masuquul Haque,^[a] and Sung Hwa Jung*^[a]

Keywords: Metal-organic frameworks / Lability / Ultrasound / Synthetic methods / Kinetics

Porous isostructural [Ln(BTC)(H₂O)·4.3H₂O], or Ln–BTC (Ln: Ce, Tb, and Y; BTC stands for 1,3,5-benzenetricarboxylate), with a tetragonal structure has been synthesized by ultrasonic irradiation at room temperature. Under ultrasound, the syntheses were quickly accelerated to obtain the fully crystallized phase in only minutes. The particle size can be considerably decreased by this method. On the basis of XRD, field-emission scanning electron microscopy (FE-SEM), and surface area analyses, it can be understood that the Ln–BTCs are homogeneous in phase, isostructural, and microporous.

The synthesis rates are $r_{\text{Ce-BTC}} > r_{\text{Tb-BTC}} > r_{\text{Y-BTC}}$ for both in the nucleation and crystal-growth stages, thereby illustrating the importance of the lability of the metal ions in the synthesis of the metal-organic framework (MOF) materials. The Tb–BTC shows luminescence properties, a characteristic property of Tb³⁺ (green-light emission), in the range of 470–630 nm at room temperature. It is believed that these lanthanide MOFs with micropores and/or luminescent properties should be proven to be multifunctional materials on further investigations.

Introduction

The number of materials that exhibit permanent nanoporosity has rapidly expanded in recent years, due in large part to the discovery of metal-organic frameworks (MOFs).^[1] The major applications currently being considered for these compounds involve gas storage,^[2] catalysis,^[3] separations,^[4] carriers for nanomaterials,^[5] luminescence,^[6] electrode materials,^[7] magnetism,^[8] and drug delivery.^[9] For these applications, their high surface areas and unique pore structures are likely to offer many potential advantages over existing compounds.

Among the MOFs, metal carboxylates are particularly interesting because they are highly porous and are very stable in water or under ambient conditions. Generally, transition-metal carboxylates such as metal–BDCs or metal–BTCs (BTC and BDC stand for 1,3,5-benzenetricarboxylate and 1,4-benzenedicarboxylate or terephthalate, respectively) have been widely studied, whereas lanthanide (Ln)-based MOFs have been significantly less studied. However, the situation has been changing over the past few years due to the excellent optical and magnetic properties of lanthanide complexes.^[10] Moreover, the high coordination number and diverse coordination geometry of central Ln ions lead to the formation of interesting frameworks and challenging topologies.

Generally, lanthanides with abundant 4f electron configurations have been successfully used as luminescent materials. When Ln^{III} is embedded into a ligand or host lattice, the 4fⁿ ground configuration and 4f^{n–1}–5d excited configuration of Ln^{III} introduce excitation and emission spectra. Ln-based MOFs with light-emitting and magnetic properties are now considered very important because of their versatile applications. Very recently, Ln-based MOFs have attracted considerable attention due to the possibility of designing the frameworks from multifunctional ligands and Ln ions, thereby achieving a successful outcome in the synthesis of porous frameworks with adsorption/storage, luminescence, and magnetic properties, and so on.^[11] Tb–BTC, called MOF-76, one of the typical Ln–BTCs, was reported by Rosi et al.^[12a] The luminescence and sensing properties of Tb–BTC have also been studied by Chen et al.^[12b] and Xiao et al.^[12c] Another Ln–BTC, Y–BTC [Y(BTC)(H₂O)·4.3H₂O], was reported by Luo et al.^[13] They have shown that a tetragonal porous framework, Y–BTC, with an optimal pore size of approximately 6 Å, is a promising candidate for hydrogen storage. It has been reported that at high concentration of hydrogen loading, Y–BTC is able to hold hydrogen molecules up to 3.7 wt.-%.

There are several examples of the synthesis of MOFs with the same crystal structure for different transition-metal ions. Transition-metal BDCs such as MIL-53(Al, Cr, Fe) and MIL-47(V) are well known for their isostructure with different metal ions.^[14] MIL-100 has also been obtained from Cr, Al, and Fe ions.^[15] Hydrogen adsorption on various isostructural MOFs, Me₂(2,5-dihydroxyterephthalate) (Me: Mg, Co, Ni, Zn), has been studied.^[16] MIL-96^[17] or MIL-122^[18] can be produced from Al, Ga, and In. Like

[a] Department of Chemistry, Kyungpook National University, Daegu 702-701, Korea
Fax: +82-53-950-6330
E-mail: sung@knu.ac.kr

Supporting information for this article is available on the WWW under <http://dx.doi.org/10.1002/ejic.201000541>.

transition-metal ions, the isostructural formation of MOFs from different Ln ions with different characteristic properties has been reported very recently.^[10d,11d,12c,13] Various Ln-1,3,5-benzenetrisbenzoates with a high surface area have been reported by Devic et al.^[11h]

The formation of isostructural complexes/MOFs can be explained by the similar coordination number and geometry of the Ln ions towards the ligands; however, the comparative study of Ln ions for complexation has not been studied so far. Detailed synthesis of isostructural Ln-MOFs under wide reaction conditions may increase understanding of the synthesis. It will also be interesting to compare the synthesis kinetics of Ln-MOFs with that of transition-metal MOFs^[14e,19] and inorganic porous materials^[20] such as zeolites and aluminophosphates because it has been known that kinetics is important in the synthesis of inorganic porous materials, especially syntheses that take place in reduced time.

Various MOFs have generally been synthesized widely by slow diffusion techniques, and conventional hydrothermal and solvothermal methods.^[1] However, the reactions used to synthesize many MOFs, particularly those with good thermal stability, require hydro/solvothermal synthesis conditions. Since hydro/solvothermal reactions typically need up to several days, it is important to develop facile, rapid, inexpensive, and commercially viable routes to the production of these compounds for them to be considered for applications. To find effective alternative methods for the synthesis of MOFs, a few new techniques have been explored with a view to decreasing the reaction time or reaction temperature. For example, ultrasound (US) has been applied in the synthesis of $\text{Cu}_3(\text{BTC})_2$ (Cu-BTC or HKUST-1),^[21] $\text{Zn}_3(\text{BTC})_2 \cdot 12\text{H}_2\text{O}$,^[22] $[\text{Zn}(\text{BDC})(\text{H}_2\text{O})]_n$,^[23] Fe-BDC,^[19c] and MOF-5.^[24] This method has also shown to provide an efficient way to synthesize MOFs with short crystallization time, especially with low reaction temperature and ambient pressure. Microwaves have been used for the synthesis of MOFs because microwave synthesis of porous materials has several advantages, for example, fast crystallization,^[19c,25] phase selectivity,^[26] morphology/size control,^[27] and the facile evaluation of reaction parameters.^[28] Characteristics and advantages of microwave synthesis of inorganic porous materials have been summarized in relevant reviews.^[29]

Herein, we report a time-efficient and low-temperature route to synthesize isostructural Ln-BTCs (Ln: Y, Tb, and Ce) under US with the purpose to understand the relative activity of metal-ion species in the syntheses. Relative rates in both nucleation and crystal growth for the syntheses of three Ln-MOFs were studied. Additionally, syntheses by conventional electric (CE) heating were carried out to compare the synthesis methods. The luminescent property of Tb-BTC has also been confirmed.

Results and Discussion

The reaction conditions for the synthesis of Y-BTC using CE heating have been reported recently,^[13] however,

in the present work we report the synthesis route for three isostructural Ln-BTCs (Y-, Tb-, and Ce-BTCs) with small particle size and high porosity. In our study, along with CE heating, sonication at room temperature has been introduced to decrease the reaction time and energy consumption. Figure 1 shows the XRD patterns of fully crystallized Tb-, Ce-, and Y-BTCs obtained by CE heating. In accord with the previous work for the synthesis of Y-BTC,^[13] all the diffraction peaks matched exactly with the peaks of the simulated Y-BTC, and no additional peak of impurities was detected, which clearly suggests that Tb- and Ce-BTCs are pure and isostructural to the Y-BTC structure.

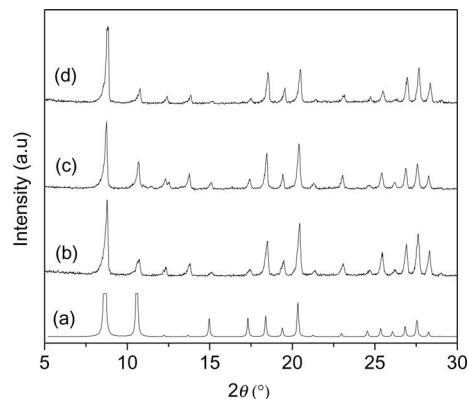


Figure 1. XRD patterns of fully crystallized and simulated Ln-BTCs: (a) simulated Y-BTC; (b) Y-BTC, (c) Tb-BTC, and (d) Ce-BTC obtained by conventional electric (CE) heating for 720 min at 100 °C.

Figure 2 shows the XRD patterns of fully crystallized Tb-BTCs synthesized by conventional heating and a sonochemical method. The result of the XRD patterns suggests that a pure Tb-BTC can be synthesized by a sonochemical method even at room temperature and in a very short time. It is observed that fully crystallized Tb-BTC is synthesized in 12 h at 100 °C by CE heating, whereas the synthesis is completed in 20 min at room temperature with US. From this result, it is clear that the rate of syntheses under US is much higher than that under CE heating. Rapid synthesis of a MOFs (Fe-BDC,^[19c] Cu-BTC^[21]) under ultrasound has been reported very recently. The XRD patterns of other Ln-BTCs obtained by US are shown in Figure S1 of the Supporting Information. Generally, porous materials have been synthesized with batch processes due to long reaction time and high reaction temperature, thereby preventing a continuous production.^[31] The facile and rapid synthesis by an ultrasonic method may lead to a continuous production of Ln-BTCs.

So far very little comprehensive study has been made to explain why the synthesis time is drastically decreased under US irradiation. The acceleration observed under US conditions in many synthetic reactions has been explained by “acoustic cavitation,”^[32] the process composed of the formation, growth, and implosive collapse of micrometer-sized bubbles under US conditions. Local conditions during bubble implosion lead to hot spots with temperatures of around 5000 °C, pressures of around 1000 atm, and extraordinary

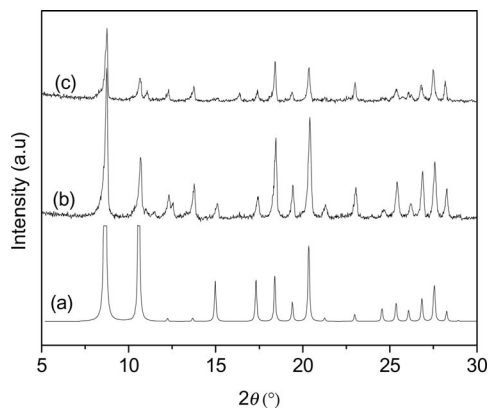


Figure 2. XRD patterns of fully crystallized and simulated Ln-BTCs: (a) simulated Y-BTC; (b) Tb-BTC synthesized by CE heating for 720 min at 100 °C, and (c) Tb-BTC synthesized by US irradiation for 20 min at room temperature.

high heating/cooling rates of approximately $10^{10} \text{ °C s}^{-1}$.^[32] Therefore, various reactions can be accelerated even at room temperature under US conditions because the instantaneous temperature and pressure may be very high. Thus, the acceleration observed in MOF syntheses may be explained with physical effects^[19c] such as hot spots or transient temperature and pressure.

The field-emission scanning electron microscopy (FE-SEM) images in Figure 3 show that the fully crystallized Tb-BTC obtained by CE heating is composed of relatively big particles (15–20 μm), whereas sonication leads to small and homogeneous particles (2–3 μm). The FE-SEM images of Ce- and Y-BTCs (presented in Figure S2 in the Supporting Information) also show that the morphologies of both Ln-BTCs are similar to that of Tb-BTCs. In this study, it can be found that sonication is a very effective way to synthesize small and homogeneous particles. Synthesis of small and homogeneous Fe-BDC^[19c] and Cu-BTC^[21b] under ultrasound has also been reported very recently.

The shape and size of porous materials are very important for applications such as catalysis, adsorption, and separation.^[33] The importance of nanoscale MOFs in magnetic resonance imaging and drug delivery has also been reported very recently.^[34] Moreover, small particles are also effective in the preparation of membranes or films. The morphologies, especially under US, are very homogeneous, which shows the purity of the crystallized phase and the efficiency of the synthesis method. The FE-SEM images of Ln-BTCs obtained by CE heating are not so homogeneous, probably because concomitant nucleation and crystal growth occurs under CE heating.^[20b]

The nitrogen-adsorption isotherms of fully crystallized Tb-BTCs synthesized by a CE heating and a US method shown in Figure 4 are typical of type I, which illustrates the microporosity and successful synthesis of the porous Tb-BTCs. However, the BET surface area and micropore volume of Tb-BTC obtained by the US method ($678 \text{ m}^2 \text{ g}^{-1}$ and $0.25 \text{ cm}^3 \text{ g}^{-1}$) are higher than those of the sample obtained by CE heating ($535 \text{ m}^2 \text{ g}^{-1}$ and $0.20 \text{ cm}^3 \text{ g}^{-1}$). The im-

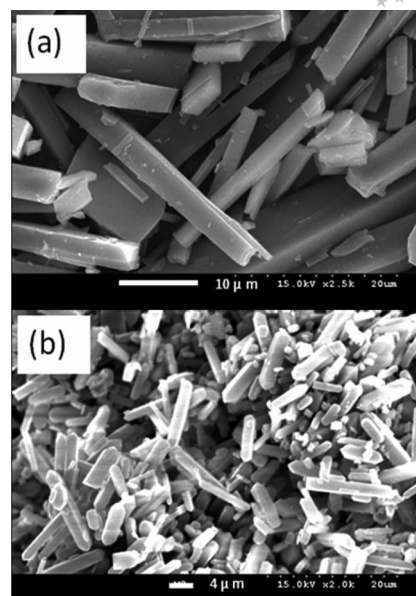


Figure 3. FE-SEM images of Tb-BTCs obtained by (a) CE heating for 720 min at 100 °C and (b) US irradiation for 20 min at room temperature.

proved surface area and micropore volume for the sonicated sample are probably due to reduced size and homogeneity of the particles (or clogged pore structure of big crystals obtained with CE heating). The nitrogen-adsorption isotherms of Ce- and Y-BTCs synthesized by both CE heating and sonication (which are shown in Figure S3 of the Supporting Information) also show the permanent porosity, and represent a similar trend of high porosity of the US-synthesized samples with small particle sizes.

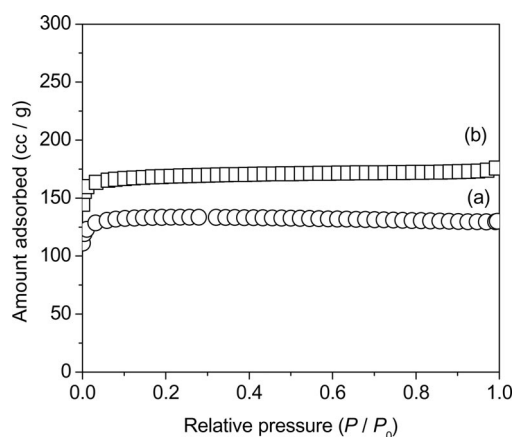


Figure 4. Nitrogen-adsorption isotherms of Tb-BTCs obtained by (a) CE heating for 720 min at 100 °C and (b) US irradiation for 20 min at room temperature.

To understand the relative lability of lanthanides (Tb^{III} , Ce^{III} , and Y^{III}) in the synthesis of Ln-BTCs, both the rates of nucleation and crystal growth were compared. In our study, room-temperature syntheses by using US were chosen for this purpose. Figure 5 shows the XRD patterns of isostructural Ln-BTCs (with three different metal centers, Y^{III} , Tb^{III} , and Ce^{III}) synthesized at room temperature by

US irradiation for various reaction times. As shown in the figure, the XRD intensity increases with increasing reaction time and saturates at a certain point in time. There is no noticeable change of the intensity with a further increase in the reaction time. Quantitative accelerations on both nucleation and crystal growth were calculated from the crystallization curve of Figure 6. The time of the first appearance of XRD peaks (Figure 5) and the slope of crystallization curves (between 20 and 80% of fully crystallized Ln–BTCs)

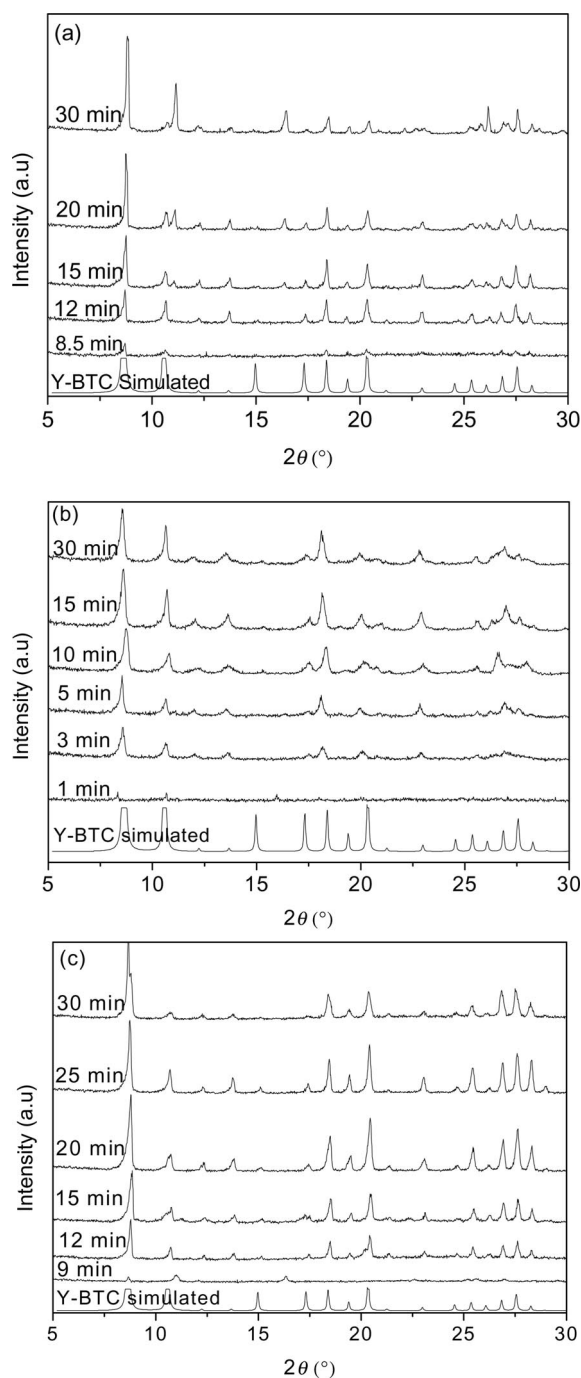


Figure 5. Change in the XRD patterns of (a) Tb–BTCs, (b) Ce–BTCs, and (c) Y–BTCs synthesized by US irradiation with an increase in reaction times at room temperature.

were utilized to determine the rate of nucleation and crystal growth, respectively.^[30] The time needed for complete nucleation (or induction period) and the rates of nucleation and crystal growth depending on the three different metals are summarized in Table 1. It was found that nucleation and crystallization (up to 100%) take 1.0, 9.0; 8.5, 11.5; and 9.0, 16.5 min for Ce–, Tb–, and Y–BTCs, respectively. The crystallization curve and Table 1 show that Ce^{III} is much more reactive in forming both nuclei and crystals than Tb^{III} and Y^{III}, whereas Tb^{III} shows a bit higher reactivity than Y^{III}. For the synthesis of Ce–BTC the nucleation rate is 8.3 and 9.1 times faster, and the crystal growth rate is 3.6 and 5.6 times faster than those for the synthesis of Tb– and Y–BTCs, respectively. The nucleation and crystal-growth rate for the synthesis of Tb–BTC is 1.1 and 1.6 times faster than those for the synthesis of Y–BTC. The kinetics of the syntheses depending on the metal ions is summarized in Scheme 1.

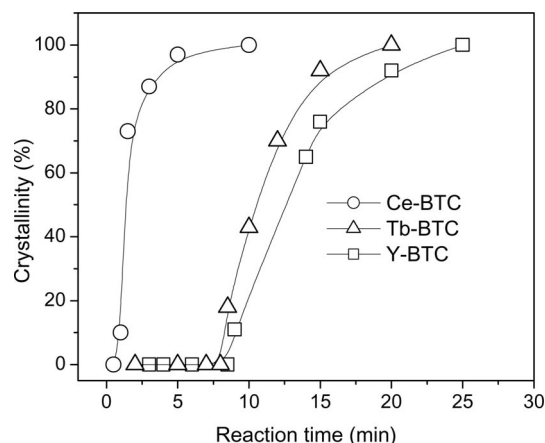


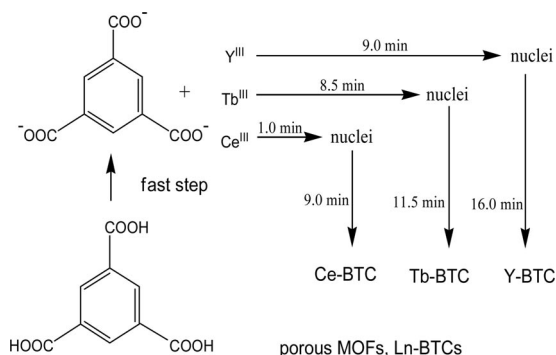
Figure 6. Crystallization curves of isostructural Ln–BTCs obtained by US irradiation at room temperature for various reaction times.

Table 1. Nucleation and crystal-growth rates of three Ln–BTCs obtained by US irradiation at room temperature.

La–BTCs	Nucleation time [min]	Nucleation rate ^[a] [min ^{−1}]	Crystal-growth rate ^[b] [min ^{−1}]
Ce–BTC	1.0	1.00	0.50
Tb–BTC	8.5	0.12	0.14
Y–BTC	9.0	0.11	0.09

[a] Calculated from the inverse of the nucleation time. [b] Calculated from the slope of a crystallization curve (between 20 and 80% crystallinity).

From this result, it can be assumed that the rate of deprotonation of trimesic acid to BTC is faster than the complexation to form MOFs because the lability of metal ions controls the reaction rate. If the deprotonation is slow and is the rate-determining step, the lability of metal ions does not have a noticeable effect on the synthesis rate. The fast deprotonation is probably due to the presence of *N,N*-dimethylformide (a weak base) in the reaction mixture. Similar results of rapid deprotonation, even in acidic conditions, were also observed in the synthesis of transition-metal-based MOFs.^[14e,35] The higher reactivity or lability



Scheme 1. Synthesis of porous Ln-BTCs (Ln: Tb, Ce, and Y).

of Ce^{III} among the three metal cations can be explained with the rate of the water-exchange reaction.^[36] Generally, compared with Y^{III} and Tb^{III} , Ce^{III} is considered to be a labile ion in kinetics due to a small ligand-field stabilization energy.^[36] The rate constants for the water-exchange reaction are also $\text{Ce}^{\text{III}} \gg \text{Tb}^{\text{III}} > \text{Y}^{\text{III}}$.^[36] The synthesis rate of the three Ln-BTCs, therefore, correlates well with the lability of metal ions, thus showing the importance of lability or inertness of metal ions in the synthesis rates of MOFs due to the simple process of complexation or ligand exchange in MOFs synthesis.

The luminescent properties of Tb-BTC are shown in Figure 7. The excitation spectrum of Tb^{3+} monitored at

542 nm is shown in part b of Figure 7. This spectrum consists of a broad band and some sharp peaks. The broad band in the range of 250 to 300 nm is due to the charge-transfer (CT) band between the ligand and metal ion (O^{2-} to Tb^{3+}). On the other hand, the sharp peaks in the range of 300–500 nm are due to the f–f transitions of Tb^{3+} . From this figure, it can be understood that the excitation due to the CT band is the dominant peak and the maximum excitation intensity is situated at 290 nm. The emission profile/spectrum of Tb-BTC with an excitation wavelength at 290 nm is shown in Figure 7 (a). The typical emission of Tb^{3+} is observed in the measured spectrum. The strongest emission peak is located at about 542 nm, which is due to the $^5\text{D}_4$ to $^7\text{F}_5$ transition of Tb^{3+} . The other peaks can be assigned due to the transitions of the $^5\text{D}_4$ level to $^7\text{F}_J$ ($J = 3, 4$, and 6) levels of Tb^{3+} . The luminescent properties of this study is very similar to the Tb-BTC reported by Chen and Xiao et al.^[12b,12c] The intense green emission and good excitation profile of Tb-BTC may suggest its possibility as a promising luminescent material for high-efficiency fluorescent lamps and other practical purposes.

Conclusion

Isostructural Ln-BTCs (Ln: Ce, Tb, and Y) metal-organic framework materials (MOFs) can be readily synthesized under ultrasonic irradiation within minutes at room temperature and ambient pressure. The synthesized Ln-BTCs under ultrasonic irradiation show relatively small and homogeneous particles, and improved surface area and pore volume compared with conventional synthesis at high temperature. The synthesis rate of the Ln-BTCs under US, irrespective of the synthesis stages (nucleation and crystal growth), is $r_{\text{Ce-BTC}} > r_{\text{Tb-BTC}} > r_{\text{Y-BTC}}$ and the rate correlates well with the lability of the metal ions. The observed reaction rate suggests the importance of lability/inertness of a metal ion in the kinetics of MOFs synthesis due to the simple process of complexation or ligand exchange in the synthesis. Moreover, Tb-BTC exhibits green-light emission in the range of 470–630 nm at room temperature. It is believed that these lanthanide MOFs with micropores and/or luminescent properties should be proven to be multifunctional materials on further investigations.

Experimental Section

An exact amount of trimesic acid (H_3BTC , 0.25 mmol) and $\text{Tb}(\text{NO}_3)_3 \cdot 5\text{H}_2\text{O}$ (Aldrich, 99.9%, 0.5 mmol), $\text{Ce}(\text{NO}_3)_3 \cdot 6\text{H}_2\text{O}$ (Aldrich, 99.9%, 0.5 mmol), or $\text{Y}(\text{NO}_3)_3 \cdot 6\text{H}_2\text{O}$ (Aldrich, 99.9%, 0.5 mmol) was dissolved in a solvent mixture of *N,N*-dimethylformamide (DMF, 4.0 mL) and H_2O (4.0 mL) in a sample vial at room temperature and stirred magnetically for 10 min. The vial was set to the probe of an ultrasonic (US) generator (VCX 750, Sonics & Materials, Inc). The energy of the US was kept at 20% of the maximum power (750 W) throughout the entire synthesis time. The temperature was maintained around 25 °C up to 5 min and was less than 40 °C even after sonication for 30 or 60 min due to natural cooling. In the case of CE heating, the reactant mixture was loaded

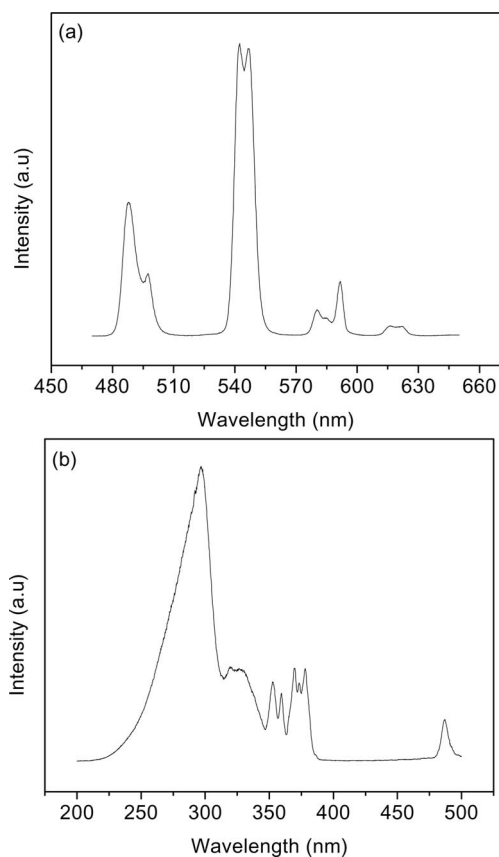


Figure 7. (a) The emission spectrum of Tb-BTC excited at 290 nm and (b) the excitation spectrum of Tb-BTC at room temperature.

in specific Teflon-lined autoclaves, sealed, and placed in a preheated electric oven for a fixed time. After finishing the reactions, the vials or the autoclaves were allowed to cool down to room temperature and the solid products were recovered with centrifugation. The solid products were washed with a water/ethanol mixture (1:1 v/v) to remove the unreacted H₃BTC and soaked in methanol for 24 h, and the extract was discarded. Fresh methanol was subsequently added. To remove solvated methanol, the sample was then treated similarly with dichloromethane. Dichloromethane was removed by decanting and the sample was calcined at 350 °C for 12 h.

The phase and crystallinity of the samples were determined with an X-ray diffractometer (MO3X-HF, model no. 1031; Cu-K α radiation). The relative rates of nucleation and crystal growth were estimated by the reciprocal of the induction period and the slope of the crystallization curve (crystallinity between 20 and 80%), respectively, similar to the reported methods.^[30] The induction period or nucleation time is the time required to observe any crystallinity (XRD intensity of 0–5% to the fully crystallized samples).^[30]

The crystal morphology was examined using a field-emission scanning electron microscope (Hitachi, S-4300). The nitrogen-adsorption isotherms were measured at –196 °C with an adsorption unit (Micromeritics, Tristar II 3020) after evacuation of the obtained samples at 150 °C for 12 h. The surface areas and micropore volumes were obtained using the BET equation and *t* plot, respectively. The emission and excitation spectra of Tb–BTC were recorded at room temperature with a Hitachi F-4500 fluorescence spectrophotometer with a 450-W xenon lamp as excitation source.

Supporting Information (see also the footnote on the first page of this article): XRD patterns, FE-SEM images, and nitrogen adsorption isotherms of both Y- and Ce–BTCs.

Acknowledgments

This work was supported by the Mid-Career Researcher Program through a National Research Fund (NRF) grant by the Ministry of Education, Science and Technology (MEST) (R01-2008-0055718, 2009-0083696).

- [1] a) O. M. Yaghi, M. O'Keeffe, N. W. Ockwig, H. K. Chae, M. Eddaoudi, J. Kim, *Nature* **2003**, *423*, 705–714; b) G. Férey, C. Mellot-Draznieks, C. Serre, F. Millange, *Acc. Chem. Res.* **2005**, *38*, 217–225; c) S. Kitagawa, R. Kitaura, S.-I. Noro, *Angew. Chem.* **2004**, *116*, 2388–2430; *Angew. Chem. Int. Ed.* **2004**, *43*, 2334–2375; d) G. Férey, *Chem. Soc. Rev.* **2008**, *37*, 191–241; e) S. Ma, *Pure Appl. Chem.* **2009**, *81*, 2235–2251; f) S. Natarajan, P. Mahata, *Chem. Soc. Rev.* **2009**, *38*, 2304–2318.
- [2] a) X. Zhao, B. Xiao, A. Fletcher, K. M. Thomas, D. Bradshaw, M. J. Rosseinsky, *Science* **2004**, *306*, 1012–1015; b) M. Dincă, J. R. Long, *J. Am. Chem. Soc.* **2005**, *127*, 9376–9377; c) J. L. C. Rowsell, E. C. Spencer, J. Eckert, J. A. K. Howard, O. M. Yaghi, *Science* **2005**, *309*, 1350–1354; d) L. J. Murray, M. Dincă, J. R. Long, *Chem. Soc. Rev.* **2009**, *38*, 1294–1314; e) M. Eddaoudi, J. Kim, N. Rosi, D. Vodak, J. Wachter, M. O'Keeffe, O. M. Yaghi, *Science* **2002**, *295*, 469–472; f) S. Bournelly, P. L. Llewellyn, C. Serre, F. Millange, T. Loiseau, G. Férey, *J. Am. Chem. Soc.* **2005**, *127*, 13519–13521.
- [3] a) A. Corma, H. Garcia, F. X. Xamena, *Chem. Rev.* **2010**, *110*, 4606–4655; b) D. Farrusseng, S. Aguado, C. Pinel, *Angew. Chem.* **2009**, *120*, 7638–7649; *Angew. Chem. Int. Ed.* **2009**, *48*, 7502–7513; c) L. Ma, C. Abney, W. Lin, *Chem. Soc. Rev.* **2009**, *38*, 1248–1256; d) J. Lee, O. K. Farha, J. Roberts, K. A. Scheidt, S. T. Nguyen, J. T. Hupp, *Chem. Soc. Rev.* **2009**, *38*, 1450–1459.
- [4] a) H. Deng, C. J. Doonan, H. Furukawa, R. B. Ferreira, J. Towne, C. B. Knobler, B. Wang, O. M. Yaghi, *Science* **2010**, *327*, 846–850; b) S. Ma, D. Sun, X.-S. Wang, H.-C. Zhou, *Angew. Chem.* **2007**, *119*, 2510–2514; *Angew. Chem. Int. Ed.* **2007**, *46*, 2458–2462; c) J.-R. Li, R. J. Kuppler, H.-C. Zhou, *Chem. Soc. Rev.* **2009**, *38*, 1477–1504; d) L. Alaerts, C. E. A. Kirschhock, M. Maes, M. A. van der Veen, V. Finsy, A. Depla, J. A. Martens, G. V. Baron, P. A. Jacobs, J. F. M. Denayer, D. E. De Vos, *Angew. Chem.* **2007**, *119*, 4371–4375; *Angew. Chem. Int. Ed.* **2007**, *46*, 4293–4297; e) V. Finsy, H. Verelst, L. Alaerts, D. E. De Vos, P. A. Jacobs, G. V. Baron, J. F. M. Denayer, *J. Am. Chem. Soc.* **2008**, *130*, 7110–7118; f) L. Alaerts, M. Maes, L. Giebeler, P. A. Jacobs, J. A. Martens, J. F. M. Denayer, C. E. A. Kirschhock, D. E. De Vos, *J. Am. Chem. Soc.* **2008**, *130*, 14170–14178; g) Kitaura, K. Seki, G. Akiyama, S. Kitagawa, *Angew. Chem.* **2003**, *115*, 444–447; *Angew. Chem. Int. Ed.* **2003**, *42*, 428–431; h) K. A. Cychoz, A. G. Wong-Foy, A. J. Matzger, *J. Am. Chem. Soc.* **2008**, *130*, 6938–6939; i) K. A. Cychoz, A. G. Wong-Foy, A. J. Matzger, *J. Am. Chem. Soc.* **2009**, *131*, 14538–14543.
- [5] a) M. P. Suh, H. R. Moon, E. Y. Lee, S. Y. Jang, *J. Am. Chem. Soc.* **2006**, *128*, 4710–4718; b) S. Hermes, F. Schroder, R. Chelmoski, C. Woll, R. A. Fischer, *J. Am. Chem. Soc.* **2005**, *127*, 13744–13745; c) C. Zlotea, R. Campesi, F. Cuevas, E. Leroy, P. Dibandjo, C. Volkringer, T. Loiseau, G. Férey, M. Latroche, *J. Am. Chem. Soc.* **2010**, *132*, 2991–2997.
- [6] a) M. D. Allendorf, C. A. Bauer, R. K. Bhakta, R. J. T. Houk, *Chem. Soc. Rev.* **2009**, *38*, 1330–1352; b) B. V. Harbuzaru, A. Corma, F. Rey, P. Atienzar, J. L. Jord, H. Garcia, D. Ananias, L. D. Carlos, J. Rocha, *Angew. Chem.* **2008**, *120*, 1096–1099; *Angew. Chem. Int. Ed.* **2008**, *47*, 1080–1083; c) D. T. De Lill, N. S. Gunning, C. L. Cahill, *Inorg. Chem.* **2005**, *44*, 258–266; d) Z. Li, G. Zhu, X. Guo, X. Zhao, Z. Jin, S. Qiu, *Inorg. Chem.* **2007**, *46*, 5174–5178; e) Y.-B. Dong, P. Wang, J.-P. Ma, X.-X. Zhao, H.-Y. Wang, B. Tang, R.-Q. Huang, *J. Am. Chem. Soc.* **2007**, *129*, 4872–4873; f) P. Wang, J.-P. Ma, Y.-B. Dong, *Chem. Eur. J.* **2009**, *15*, 10432–10445; g) Y.-Y. Jiang, S.-K. Ren, J.-P. Ma, Q.-K. Liu, Y.-B. Dong, *Chem. Eur. J.* **2009**, *15*, 10742–10746.
- [7] a) G. Férey, F. Millange, M. Morerette, C. Serre, M.-L. Doublet, J. M. Grenèche, M. L. Doublet, J. M. Tarascon, *Angew. Chem.* **2007**, *119*, 3323–3327; *Angew. Chem. Int. Ed.* **2007**, *46*, 3259–3263; b) C. Combettes, M. B. Yahia, L. Pedesseau, M.-L. Doublet, *J. Phys. Chem. C* **2010**, *114*, 9518–9527.
- [8] a) M. Kurmoo, *Chem. Soc. Rev.* **2009**, *38*, 1353–1379; b) S. M. Humphrey, R. A. Mole, R. I. Thompson, P. T. Wood, *Inorg. Chem.* **2010**, *49*, 3441–3448; c) X. Feng, J. Zhao, B. Liu, L. Wang, S. Ng, G. Zhang, J. Wang, X. Shi, Y. Liu, *Cryst. Growth Des.* **2010**, *10*, 1399–1408.
- [9] a) P. Horcajada, C. Serre, M. Vallet-Regi, M. Sebban, F. Taulelle, G. Férey, *Angew. Chem.* **2006**, *118*, 6120–6124; *Angew. Chem. Int. Ed.* **2006**, *45*, 5974–5978; b) P. Horcajada, C. Serre, G. Maurin, N. A. Ramsahye, F. Balas, M. Vallet-Regi, M. Sebban, F. Taulelle, G. Férey, *J. Am. Chem. Soc.* **2008**, *130*, 6774–6780; c) W. J. Rieter, K. M. L. Taylor, H. An, W. Lin, W. Lin, *J. Am. Chem. Soc.* **2006**, *128*, 9024–9025; d) R. C. Huxford, J. D. Rocca, W. Lin, *Curr. Opin. Chem. Biol.* **2010**, *14*, 262–268; e) J. An, S. J. Geib, N. L. Rosi, *J. Am. Chem. Soc.* **2009**, *131*, 8376–8377.
- [10] a) B. Q. Ma, D. S. Zhang, S. Gao, T. Z. Jin, C. H. Yan, G. X. Xu, *Angew. Chem.* **2000**, *112*, 3790–3792; *Angew. Chem. Int. Ed.* **2000**, *39*, 3644–3646; b) N. M. Shavaleev, G. Accorsi, D. Virgili, Z. Bell, T. Lazarides, G. Calogero, N. Armaroli, M. D. Ward, *Inorg. Chem.* **2005**, *44*, 61–72; c) X. D. Guo, G. S. Zhu, F. X. Sun, Z. Y. Li, X. J. Zhao, X. T. Li, H. C. Wang, S. L. Qiu, *Inorg. Chem.* **2006**, *45*, 2581–2587; d) B. Chen, Y. Yang, F. Zapata, G. Lin, G. Qian, E. B. Lobkovsky, *Adv. Mater.* **2007**, *19*, 1693–1696; e) C. Daiguebonne, N. Kerbellec, O. Guillo, J. C. Bünzli, F. Gumy, L. Catala, T. Mallah, N. Audebrand, Y. Gérault, K. Bernot, G. Calvez, *Inorg. Chem.* **2008**, *47*, 3700–

- 3708; f) S. C. Manna, E. Zangrando, J. Ribas, N. R. Chaudhuri, *Polyhedron* **2006**, *25*, 1779–1786; g) B. Zhai, L. Yi, H. S. Wang, B. Zhan, P. Chen, D. Z. Liao, S. P. Yan, *Inorg. Chem.* **2006**, *45*, 8471–8473; h) A. Sonnauer, C. Nther, H. A. Hppe, J. Senker, N. Stock, *Inorg. Chem.* **2007**, *46*, 9968–9974; i) G. X. Wang, G. F. Han, Q. Ye, R. G. Xiong, T. Akutagawa, T. Nakamura, P. W. H. Chen, S. D. Huang, *Dalton Trans.* **2008**, 2527–2530.
- [11] a) P. Silva, A. A. Valente, J. Rocha, F. A. A. Paz, *Cryst. Growth Des.* **2010**, *10*, 2025–2028; b) W.-H. Zhu, Z.-M. Wang, S. Gao, *Inorg. Chem.* **2007**, *46*, 1337–1342; c) D.-K. Cao, S.-Z. Hou, Y.-Z. Li, L.-M. Zheng, *Cryst. Growth Des.* **2009**, *9*, 4445–4449; d) X. Feng, J. Zhao, B. Liu, L. Wang, S. Ng, G. Zhang, J. Wang, X. Shi, Y. Liu, *Cryst. Growth Des.* **2010**, *10*, 1399–1408; e) K. A. White, D. A. Chengelis, K. A. Gogick, J. Stehman, N. L. Rosi, S. Petoud, *J. Am. Chem. Soc.* **2009**, *131*, 18069–18071; f) X.-J. Zhao, T. Ben, M. Xue, G.-S. Zhu, Q.-R. Fang, S.-L. Qiu, *J. Mol. Struct.* **2009**, *931*, 25–30; g) F. Gándara, V. A. de la P.-O'Shea, F. Illas, N. Snejkó, D. M. Proserpio, E. G.-Puebla, M. A. Monge, *Inorg. Chem.* **2009**, *48*, 4707–4713; h) T. Devic, C. Serre, N. Audebrand, J. Marrot, G. Férey, *J. Am. Chem. Soc.* **2005**, *127*, 12788–12789; i) M. J. Vitorino, T. Devic, M. Tromp, G. Férey, M. Visseaux, *Macromol. Chem. Phys.* **2009**, *210*, 1923–1932.
- [12] a) N. L. Rosi, J. Kim, M. Eddaoudi, B. Chen, M. O'Keeffe, O. M. Yaghi, *J. Am. Chem. Soc.* **2005**, *127*, 1504–1518; b) B. Chen, L. Wang, F. Zapata, G. Qian, E. B. Lobkovsky, *J. Am. Chem. Soc.* **2008**, *130*, 6718–6719; c) Y. Xiao, L. Wang, Y. Cui, B. Chen, F. Zapata, G. Qian, *J. Alloys Compd.* **2009**, *484*, 601–604.
- [13] J. Luo, H. Xu, Y. Liu, Y. Zhao, L. L. Daemen, C. Brown, T. V. Timofeeva, S. Ma, H.-C. Zhou, *J. Am. Chem. Soc.* **2008**, *130*, 9626–9627.
- [14] a) T. Loiseau, C. Serre, C. Huguenard, G. Fink, F. Taulelle, M. Henry, T. Bataille, G. Férey, *Chem. Eur. J.* **2004**, *10*, 1373–1382; b) C. Serre, F. Millange, C. Thouvenot, M. Nogués, G. Marsolier, D. Louër, G. Férey, *J. Am. Chem. Soc.* **2002**, *124*, 13519–12526; c) K. Barthelet, J. Marrot, D. Riou, G. Férey, *Angew. Chem.* **2002**, *114*, 291–294; *Angew. Chem. Int. Ed.* **2002**, *41*, 281–284; d) C. Scherb, A. Schödel, T. Bein, *Angew. Chem.* **2008**, *120*, 5861–5863; *Angew. Chem. Int. Ed.* **2008**, *47*, 5777–5779; e) E. Haque, J. H. Jeong, S. H. Jung, *CrystEngComm.* **2010**, in press (DOI: 10.1039/b927113a).
- [15] a) G. Férey, C. Serre, C. Mellot-Draznieks, F. Millange, S. Surblé, J. Dutour, I. Margiolaki, *Angew. Chem.* **2004**, *116*, 6456–6461; *Angew. Chem. Int. Ed.* **2004**, *43*, 6296–6301; b) P. Horcajada, S. Surblé, C. Serre, D.-Y. Hong, Y.-K. Seo, J.-S. Chang, J.-M. Grenèche, I. Margiolaki, G. Férey, *Chem. Commun.* **2007**, 2820–2822; c) C. Volkringer, D. Popov, T. Loiseau, G. Férey, M. Burghammer, C. Riekel, M. Haouas, F. Taulelle, *Chem. Mater.* **2009**, *21*, 5695–5697.
- [16] W. Zhou, H. Wu, T. Yildirim, *J. Am. Chem. Soc.* **2009**, *131*, 4995–5000.
- [17] a) T. Loiseau, L. Lecroq, C. Volkringer, J. Marrot, G. Férey, M. Haouas, F. Taulelle, S. Bourrelly, P. L. Llewellyn, M. Latroche, *J. Am. Chem. Soc.* **2006**, *128*, 10223–10230; b) C. Volkringer, T. Loiseau, G. Férey, C. M. Morais, F. Taulelle, V. Montouillout, D. Massiot, *Microporous Mesoporous Mater.* **2007**, *105*, 111–117; c) C. Volkringer, T. Loiseau, *Mater. Res. Bull.* **2006**, *41*, 948–954.
- [18] C. Volkringer, T. Loiseau, N. Guillou, G. Férey, E. Elkaïm, *Solid State Sci.* **2009**, *11*, 1507–1512.
- [19] a) A. K. Cheetham, C. N. R. Rao, R. K. Feller, *Chem. Commun.* **2006**, 4780–4795; b) N. A. Khan, E. Haque, S. H. Jung, *Phys. Chem. Chem. Phys.* **2010**, *12*, 2625–263; c) E. Haque, N. A. Khan, J. H. Park, S. H. Jung, *Chem. Eur. J.* **2010**, *16*, 1046–1052.
- [20] a) M. Gharibeh, G. A. Tompsett, W. C. Conner, *Top. Catal.* **2008**, *49*, 157–166; b) S. H. Jung, T. Jin, Y. K. Hwang, J.-S. Chang, *Chem. Eur. J.* **2007**, *13*, 4410–4417.
- [21] a) Z.-Q. Li, L.-G. Qiu, T. Xu, Y. Wu, W. Wang, Z.-Y. Wu, X. Jiang, *Mater. Lett.* **2009**, *63*, 78–80; b) N. A. Khan, S. H. Jung, *Bull. Korean Chem. Soc.* **2009**, *30*, 2921–2926.
- [22] L.-G. Qiu, Z.-Q. Li, Y. Wu, T. Xu, X. Jiang, *Chem. Commun.* **2008**, 3642–3644.
- [23] Z.-Q. Li, L.-G. Qiu, W. Wang, T. Xu, Y. Wu, X. Jiang, *Inorg. Chem. Commun.* **2008**, *11*, 1375–1377.
- [24] W.-J. Son, J. Kim, J. Kim, W.-S. Ahn, *Chem. Commun.* **2008**, 47, 6336–6338.
- [25] a) X.-F. Wang, Y.-B. Zhang, H. Hang, J.-P. Zhang, X.-M. Chen, *Cryst. Growth Des.* **2008**, *8*, 4559–4563; b) S. H. Jung, J.-H. Lee, J.-S. Chang, *Bull. Korean Chem. Soc.* **2005**, *26*, 880–881; c) J. Y. Choi, J. Kim, S. H. Jung, H.-K. Kim, J.-S. Chang, H. K. Chae, *Bull. Korean Chem. Soc.* **2006**, *27*, 1523–1524; d) Z. Ni, R. I. Masel, *J. Am. Chem. Soc.* **2006**, *128*, 12394–12395.
- [26] a) N. Khan, S. H. Jung, *Cryst. Growth Des.* **2010**, *10*, 1860–1865; b) S. H. Jung, J.-H. Lee, P. M. Forster, G. Férey, A. K. Cheetham, J.-S. Chang, *Chem. Eur. J.* **2006**, *12*, 7899–7905; c) S. H. Jung, T. Jin, J.-S. Hwang, J.-S. Chang, *J. Nanosci. Nanotechnol.* **2007**, *7*, 2734–2740; d) S. H. Jung, J.-S. Chang, J.-S. Hwang, S.-E. Park, *Microporous Mesoporous Mater.* **2003**, *64*, 33–39; e) S. H. Jung, T. Jin, Y. H. Kim, J.-S. Chang, *Microporous Mesoporous Mater.* **2008**, *109*, 58–65.
- [27] a) S. H. Jung, J.-H. Lee, J. W. Yoon, C. Serre, G. Férey, J.-S. Chang, *Adv. Mater.* **2007**, *19*, 121–124; b) S. H. Jung, J. W. Yoon, Y. K. Hwang, J.-S. Chang, *Microporous Mesoporous Mater.* **2006**, *89*, 9–15; c) Y. K. Hwang, J.-S. Chang, S.-E. Park, D. S. Kim, Y.-U. Kwon, S. H. Jung, J.-S. Hwang, M.-S. Park, *Angew. Chem.* **2005**, *117*, 562–566; *Angew. Chem. Int. Ed.* **2005**, *44*, 556–560.
- [28] a) S. H. Jung, J.-S. Chang, Y. K. Hwang, J.-M. Grenèche, G. Férey, A. K. Cheetham, *J. Phys. Chem. B* **2004**, *109*, 849–850; b) S. H. Jung, J.-S. Chang, S.-E. Park, P. M. Forster, G. Férey, A. K. Cheetham, *Chem. Mater.* **2004**, *16*, 1394–1396; c) S. H. Jung, J.-S. Chang, J. W. Yoon, J.-M. Grenèche, G. Férey, A. K. Cheetham, *Chem. Mater.* **2004**, *16*, 5552–5555.
- [29] a) S.-E. Park, J.-S. Chang, Y. K. Hwang, D. S. Kim, S. H. Jung, J.-S. Hwang, *Catal. Survey. Asia* **2004**, *8*, 91–110; b) G. A. Tompsett, W. C. Conner, K. S. Yngvesson, *ChemPhysChem* **2006**, *7*, 296–319.
- [30] a) M. Gharibeh, G. A. Tompsett, W. C. Conner, K. S. Yngvesson, *ChemPhysChem* **2008**, *9*, 2580–2591; b) D. W. Breck, *Zeolite Molecular Sieves*, Wiley, New York, **1974**, pp. 333–335; c) D. Uzcátegui, G. González, *Catal. Today* **2005**, *107–108*, 901–905.
- [31] S. H. Jung, J. W. Yoon, J.-S. Hwang, S. Jin, A. K. Cheetham, J.-S. Chang, *Chem. Mater.* **2005**, *17*, 4455–4460.
- [32] a) Y. T. Didenko, K. S. Suslick, *Nature* **2002**, *418*, 394–397; b) D. J. Flannigan, K. S. Suslick, *Nature* **2005**, *434*, 52–55.
- [33] a) F. D. Renzo, *Catal. Today* **1998**, *41*, 37–40; b) Z. A. D. Lethbridge, J. J. Williams, R. I. Walton, K. E. Evans, C. W. Smith, *Microporous Mesoporous Mater.* **2005**, *79*, 339–352; c) T. O. Drews, M. Tsapatsis, *Curr. Opin. Colloid Interface Sci.* **2005**, *10*, 233–238; d) S. Qiu, J. Yu, G. Zhu, O. Terasaki, Y. Nozue, W. Pang, R. Xu, *Microporous Mesoporous Mater.* **1998**, *21*, 245–251.
- [34] a) K. M. L. Taylor, J. D. Rocca, Z. Xie, S. Tran, W. Lin, *J. Am. Chem. Soc.* **2009**, *131*, 14261–14263; b) K. M. L. Taylor, W. J. Rieter, W. Lin, *J. Am. Chem. Soc.* **2008**, *130*, 14358–14359.
- [35] N. A. Khan, J. W. Jun, S. H. Jung, *Eur. J. Inorg. Chem.* **2010**, 1043–1048.
- [36] F. A. Cotton, G. Wilkinson, *Advanced Inorganic Chemistry*, 4th ed., John Wiley & Sons, Inc., New York, **1980**, pp. 1188–1189.

Received: May 17, 2010

Published Online: September 10, 2010